Electronic Supplementary Information

Engineering of unsubstituted quinoid-like frameworks enabling a 2 V vs Li^+/Li redox voltage tunability and related derivatives

Daniele Tomerini [a,b], Carlo Gatti [c] and Christine Frayret* [a,b]

[a] Laboratoire de Réactivité et Chimie des Solides, UMR CNRS 7314, Université de Picardie Jules Verne, 33, Rue Saint-Leu, 80039 Amiens, France.

[b] Réseau sur le Stockage Electrochimique de l'Energie (RS2E), FR CNRS 3459, France.

[c] CNR-ISTM, Istituto di Scienze e Tecnologie Molecolari, via Golgi 19, 20133, Milano, Italy.

Table of contents

S1. Computational details 2
S2. Molecular geometries 3
S2.1 High-potential systems, initial state 3
S2.2 High-potential systems, reduced state 3
S2.3 Low-potential systems, initial state 4
S2.4 Low-potential systems, reduced state 5
S3. Frontier orbitals energy 5
S4. π-electron delocalization indices: HOMA and FLU 6
S4.1 HOMA index 6
S4.2 FLU index 7
S5. Lewis forms 8
S6. Atomic spin density populations 8
S7. Atomic charges according to the Bader's QTAIM framework 9
S8. Energy partitioning based on Bader's QTAIM framework 11
S9. Bridge bond lengths and delocalization indices, δ 13
References 13

S1. Computational details

Quinoid-like, (Q), (or tetracyanoquinodimethane (TCNQ)-like in a few cases) derivatives undergo a reduction process involving the formation of the semiquinone-like or reduced (TCNQ)-like radical anion ($Q^{\bullet -}$).

All geometry optimizations and energy calculations were performed with the Gaussian09 package of programs [1].

The absolute standard redox potential values, $E^{0}_{red\,(solv)}$ were extracted from the evaluation of the Gibbs free energy difference characterizing the one-electron reduction process, $\Delta G^{0}_{red(solv)}$ (see Fig. S1), as indicated by Equation (1):

$$E^{0}_{red\,(solv)} = \frac{-\left(\Delta G^{0}_{red(solv)}\right)}{F} \qquad (1)$$

where F is the Faraday's constant.

To calculate $\Delta G^{0}_{red(solv)}$, we use the following thermodynamic cycle (Born-Haber) in order to transfer all of the species involved in the reaction from the gas phase to the solution phase. Based on this thermodynamic cycle, $\Delta G^{0}_{red\,(solv)}$ can be written as:

$$\Delta G^{0}_{red\,(solv)} = G_{298K,\,solv}(Q^{-\cdot}) - G_{298K,\,solv}(Q) = EA_{gas} + \Delta G^{*}_{solv,Q^{-\cdot}} - \Delta G^{*}_{solv,Q} \qquad (2)$$

where EA_{gas} corresponds to the electron affinity in gas-phase at 298 K, $\Delta G^{*}_{solv,Q}$ and $\Delta G^{*}_{solv,Q^{-\cdot}}$ are respectively the free energy of solvation of the compound and of its reduced counterpart.

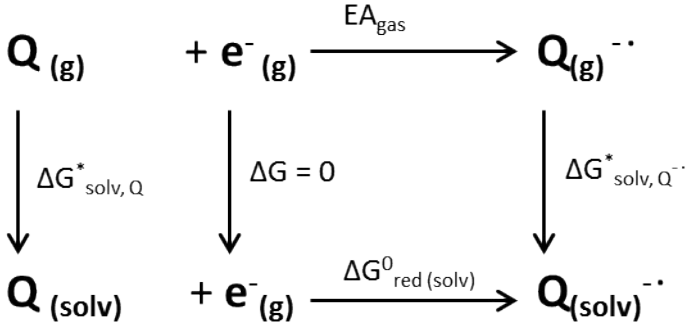

Figure S1. Thermodynamic cycle used for the estimation of the standard state free energy difference relative to the one-electron reduction process in solution, $\Delta G^{0}_{red\,(solv)}$.

For such process involving neutral (Q) and ionic radical species ($Q^{-\bullet}$) species, the SMD[2] (*solvation model* based on solute electron *density*) methodology has been chosen due to its improved description of solvation energies compared to other solvent models. Calculations carried out in solution involved Ethylene Carbonate (EC) as solvent.

The value of 1.46 V proposed by Vollmer *et al.*[3] was used to get voltages relative to the Li^{+}/Li reference electrode, according to Equation (3):

$$E^{0}_{vs\ Li/Li^{+}} = E^{0}_{red\,(solv)} - 1.46\ V \qquad (3)$$

For all DFT calculations, the 6-31+G(d,p) basis set was first applied. Geometries were fully optimized, without imposing any restriction, with the B3LYP functional (Becke's three parameter exchange functional (B3) in combination with Lee, Yang, and Parr's (LYP) correlation functions).[4,5] The final electronic energy was estimated from single-point energy calculations with the larger 6-311+G(2d,p) basis set. Local minima were ascertained by the absence of imaginary frequencies. Thermodynamic corrections at 298 K were included in the calculation of energies.

S2. Molecular geometries

S2.1 High-potential systems, initial state

The lowest energy conformation for the C=CH−CH=C molecule is planar, *trans* and centrosymmetric (Figure S2c). For the C=N−N=C molecule, it is twisted, with a torsion angle of 125.8°, (see Figure S2a). The corresponding planar conformation is significantly higher in energy (0.075 eV). For the C=CH−N=C mixed bridge type, the molecule is not completely planar (torsion angle = 175.0°), and its energy is only marginally lower than that of the planar molecule (0.008 eV).

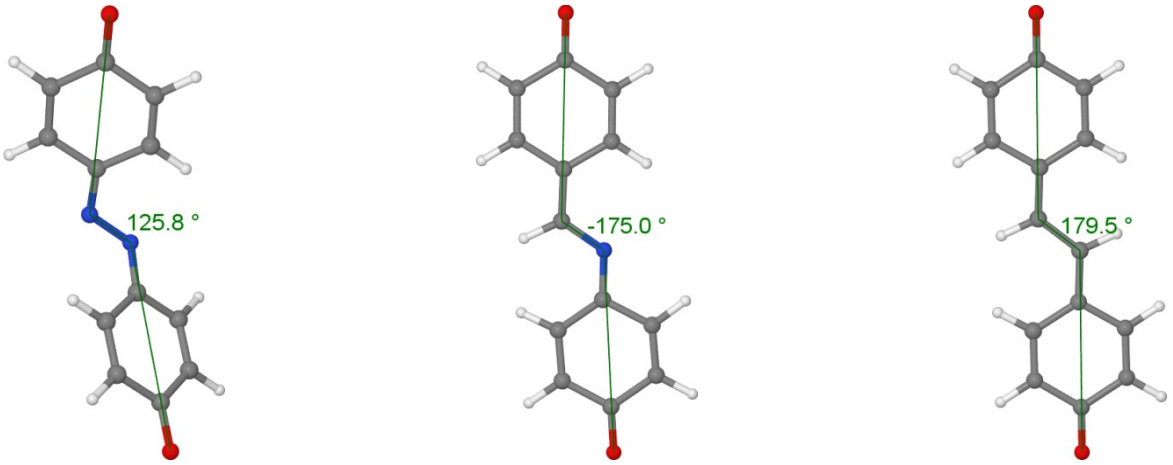

(a) C=N−N=C system **(b)** C=CH−N=C system **(c)** C=CH−CH=C system

Figure S2. Torsion angles for the high-potential C=*A*−*A(B)*=C molecules (*i.e.* at the initial state).

S2.2 High-potential systems, reduced state

For the whole set of high-potential radical anions at the reduced state, the most stable geometry (see Figure S3) is planar, exhibiting a *trans* conformation. C=*A*−*A*=C systems are centrosymmetric with respect to the central *A*−*A* bond midpoint.

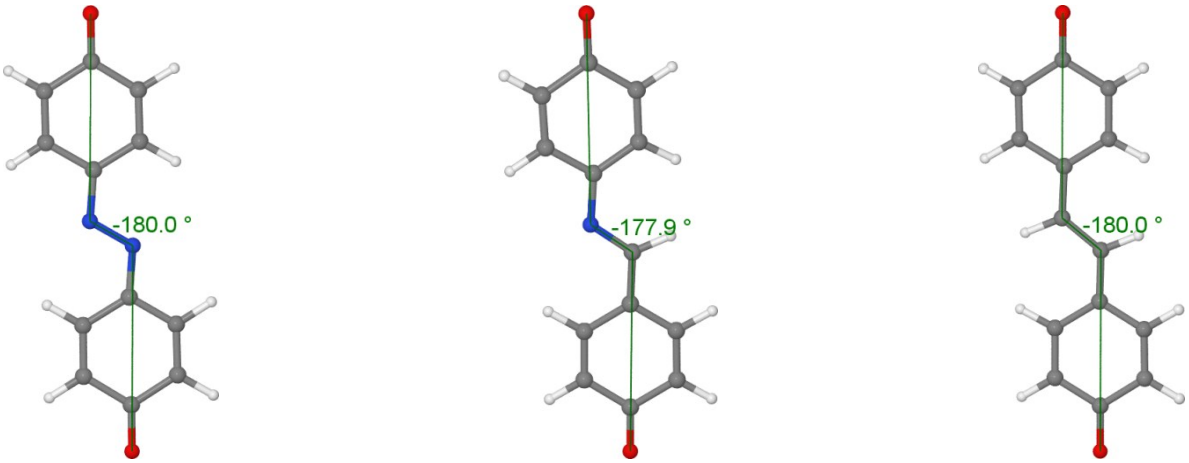

(a) C=N−N=C system **(b)** C=CH−N=C system **(c)** C=CH−CH=C system

Figure S3. Torsion angles for the high-potential C=*A*−*A(B)*=C radical anions, (*i.e.* at the reduced state).

S2.3 Low-potential systems, initial state

Contrary to the high-potential C=*A*−*A(B)*=C molecules, in low-potential CH−*X*~*X*−CH molecules (Figure S4), the possibility of a planar conformation is precluded. Except for the *X* = NH system, where the most stable conformation breaks the symmetry (Figure S4b), the stable geometries for these systems are centrosymmetric with respect to the mid-point of the *X*~*X* internuclear axis. The angle between the ring and the bridge is respectively equal to: 134.0°, ~135°, 133.3° and 128.8° for *X* = O, NH, C and CH.

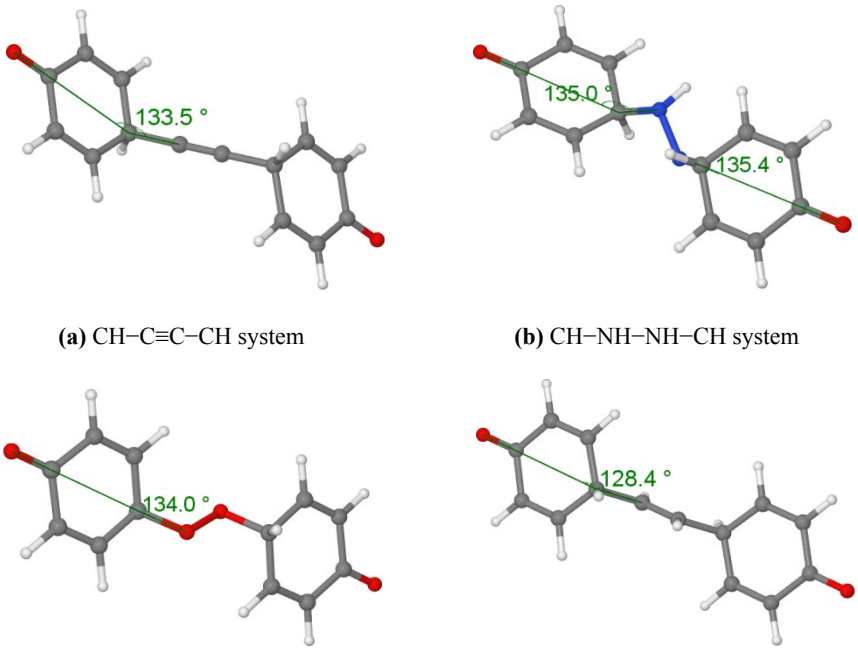

(a) CH−C≡C−CH system **(b)** CH−NH−NH−CH system

(c) CH−O−O−CH system **(d)** CH−CH=CH−CH system

Figure S4. Torsion angles in the CH−*X*~*X*−CH low-potential molecules, (*i.e.* at the initial state).

S2.4 Low-potential systems, reduced state

The reduction process introduces an asymmetry in each of the low-potential radical anion: only half of each entity exhibits significant variation of bonding and charge distribution relative to its parent initial molecule. Attempts of constraining each molecule to be symmetrical upon reduction led to higher final energies. The variation of the angle between the ring and the bridge is enhanced in the part of the molecule affected by the reduction process (Figure S5).

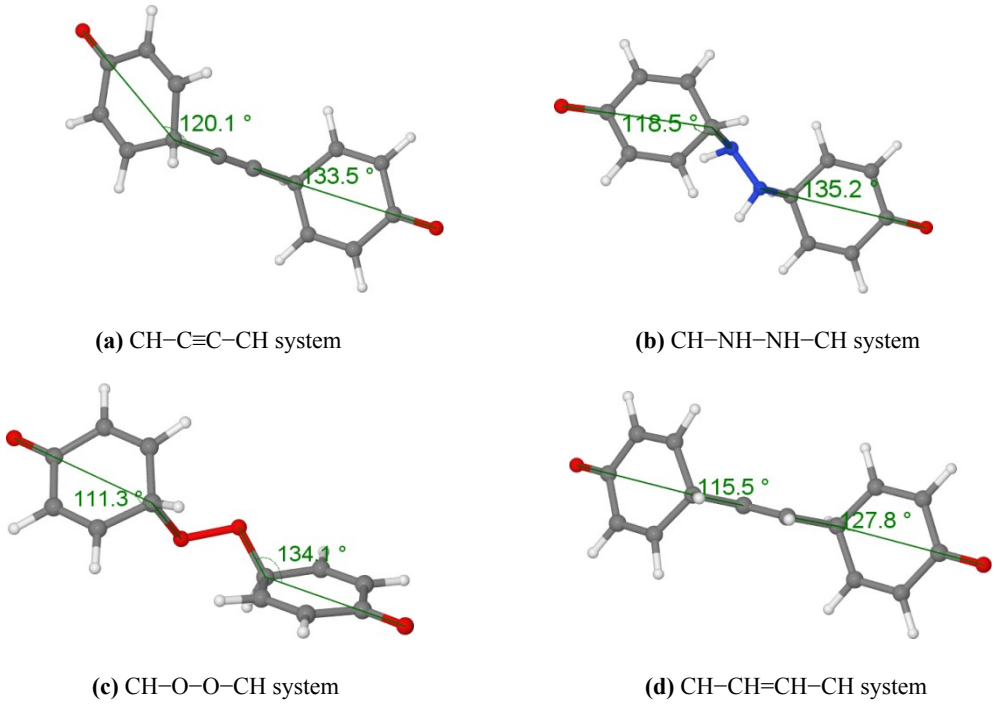

(a) CH−C≡C−CH system **(b)** CH−NH−NH−CH system

(c) CH−O−O−CH system **(d)** CH−CH=CH−CH system

Figure S5. Torsion angles in the CH−*X*~*X*−CH low-potential radical anions, (i.e. at the reduced state).

S3. Frontier orbitals energy

Calculated frontier orbitals energy, HOMO and LUMO, for the molecular initial state as well as SOMO for the radical anion in the reduced state are reported in Figure S6. The low-potential systems exhibit a marked difference between the centro-symmetric LUMO (except for *X* = NH), with delocalization over the whole entity, and the dissymmetric SOMO (whose spreading is restricted to half of the molecule).

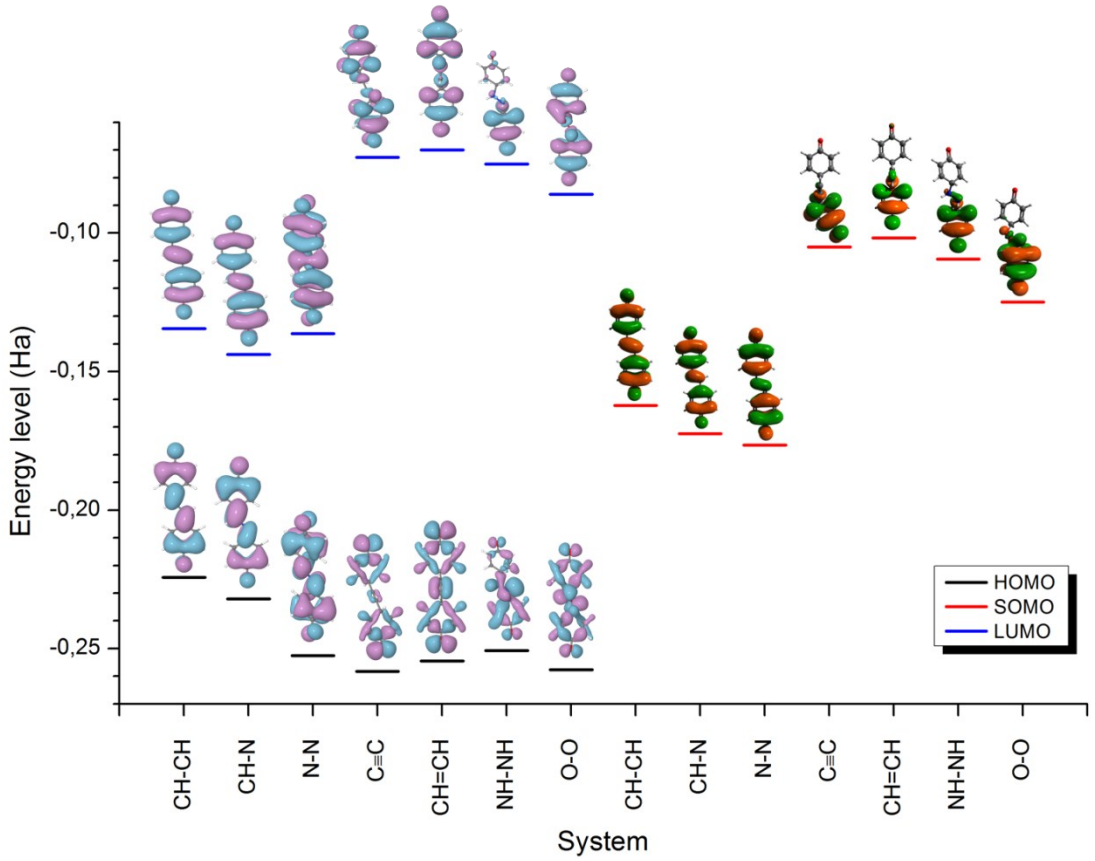

Figure S6. Relative positioning of frontier orbitals energy for the analysed systems along with corresponding topology of frontier orbitals: i.e. (HOMO/LUMO) for Q and SOMO for ($Q^{\bullet-}$) (an isocontour value of 0.02 a.u. was used).

S4. π-electron delocalization indices: HOMA and FLU

S4.1 HOMA index

The Harmonic Oscillator Model of Aromaticity index (HOMA) is a quantitative descriptor based on the geometric measure of the aromaticity. HOMA is defined as a normalized sum of squared deviations of the individual experimental (or calculated) bond lengths from an optimal value, which corresponds to full π-electron delocalization,[6] according to Equation (4):

$$HOMA = 1 - \frac{1}{N}\sum_{i=1}^{N} \propto_i (R_{opt} - R_i)^2 \qquad (4)$$

where N is the number of bonds taken into the summation; $\propto_i$ is a normalization constant fixed to give HOMA = 0 for a model non aromatic system (*e.g.* the Kekulé structure of benzene) and HOMA = 1 for the system with all bonds equal to the optimal value R_{opt} (*e.g.* a full aromatic system); R_i stands for the running bond length.

Values reported in Table S1 were estimated using the parameters: $\propto_{CC} = 257.7\ \text{Å}^{-2}$, $R_{opt,CC} = 1.388\ \text{Å}$.

System	Ring 1: HOMA values			Ring 2: HOMA values		
	Init.	Red.	Δ	Init.	Red.	Δ
N−N	-0.224	0.366	0.590			
CH−CH	0.001	0.455	0.453			
CH−N	0.018	0.421	0.403	-0.200	0.434	0.634
C≡C	-1.057	-0.912	0.145	-1.057	-1.040	0.017
CH=CH	-0.913	0.811	0.102	-0.913	0.883	0.030
NH−NH	-0.967	-0.561	0.406	-0.904	-0.902	0.002
O−O	-0.976	-0.134	0.842	-0.976	-0.946	0.030
Shortened bridge	-0.037	0.496	0.533			
C=(CN)$_2$ Red. Cent.	0.334	0.722	0.388			

Table S1. HOMA values for the rings; Ring 2 values are present for cases presenting a dissymmetry between the two rings of the system, *i.e.* Ring 2 is the ring closer to the N−bridge in C=CH−N=C molecule, while it refers to the unreduced ring in the *X*~*X* molecules).

S4.2 FLU index

The aromatic fluctuation index (FLU) (estimated here at B3LYP/6-31G(d,p) level) describes the fluctuation of electronic charge between adjacent atoms in a ring. Its expression is correlated to the two-center delocalization indices (DIs), $\delta(I,J)$, defined by Bader and co-workers which are issued from the double integration of the exchange-correlation density (one electron coordinate over I and the other over J basins). The delocalization index $\delta(I,J)$ measures the number of electrons shared between atoms I and J,[7] while $\delta_{ref}(I,J)$corresponds to the magnitude of delocalization expected for an aromatic system (*i.e.* benzene for CC bonds). The FLU index accounts for the deviation from the ideal aromatic delocalization of electronic charge over the bonds in a ring composed of C atoms and it is defined as: [8,9]

$$FLU = \frac{1}{N} \sum_{(I,J)}^{adjacent\ atoms} \left(\frac{max(V(I),V(J))}{min(V(I),V(J))} \frac{\delta(I,J) - \delta_{ref}(I,J)}{\delta_{ref}(I,J)} \right)^2 \quad (5)$$

where V is the valence of an atom in the Quantum Theory of Atoms in Molecules (QTAIM)[10] framework and where the sum is performed over the whole set of adjacent atoms I and J in the ring. $V(I)$, called the valence of atom I is instead defined as: [9]

$$V(I) = \sum_{I \neq J}^{all\ atoms} (I,J) \quad (6)$$

where now the sum runs over all atoms in the molecule.

Such calculations were performed with the Extreme and PROMEGA programs.[11]

System	Ring 1 : FLU values			Ring 2 : FLU values		
	Init.	Red.	Δ	Init.	Red.	Δ
N−N	0.062	0.033	-0.029			
CH−CH	0.143	0.124	-0.020			
CH−N	0.047	0.027	-0.020	0.060	0.028	-0.032
C≡C	0.077	0.049	-0.028	0.077	0.078	0.002
CH=CH	0.073	0.048	-0.025	0.073	0.072	0.001
NH−NH	0.080	0.060	-0.019	0.077	0.077	0.001
O−O	0.084	0.044	-0.041	0.084	0.082	-0.002
Shortened bridge	0.049	0.023	0.026			
C=(CN)$_2$ Red. Cent.	0.034	0.014	-0.020			

Table S2. FLU values for the rings; Ring 2 values are present for cases presenting a dissymmetry between the two rings of the system (Ring 2 is the ring closer to the N=C part of the bridge in C=CH−N=C system, while it refers to the unreduced ring in the *X*~*X* molecules).

S5. Lewis forms

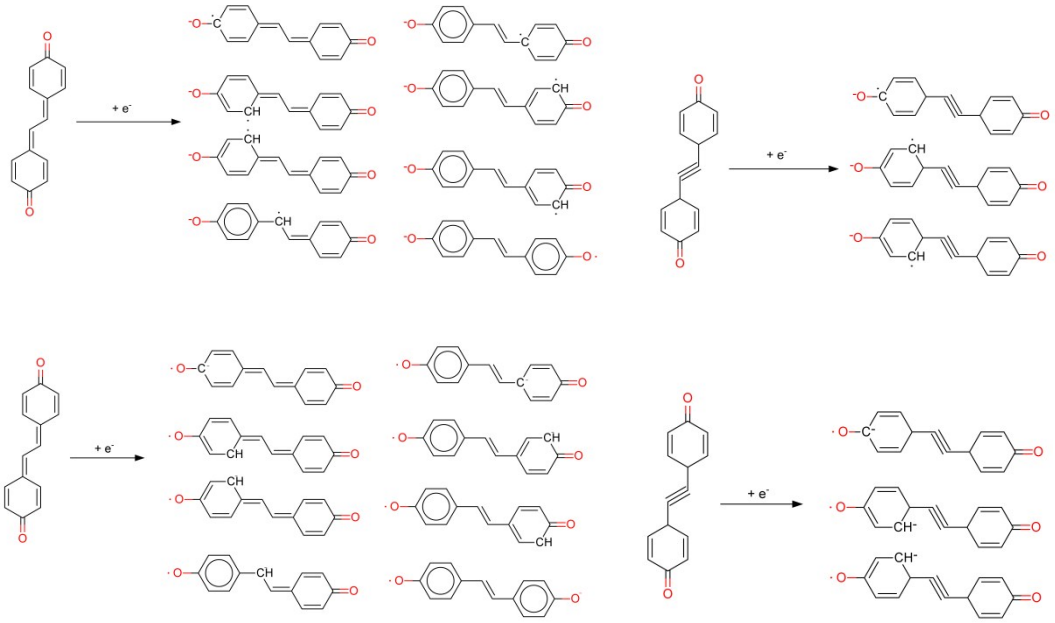

Figure S7. Lewis forms for (left): the high-potential C=CH−CH=C radical anion, and (right): the low-potential CH−C≡C−CH radical anion.

S6. Atomic spin density populations

The values of the atomic spin density populations for the whole set of radical anions corresponding to high-/low-potential systems are reported in Figures S8 and S9 respectively, in conjunction with the representation of corresponding isocontour surfaces.

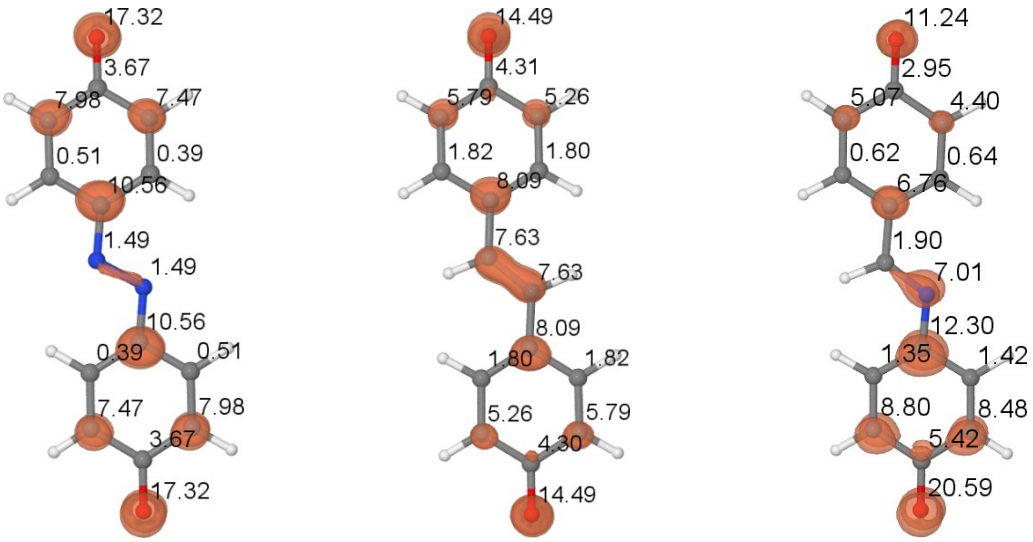

(a) C=N−N=C **(b) C=CH−CH=C** **(c) C=CH−N=C**

Figure S8. Distribution of atomic spin density population in hundredths of electron for the C=*A*−*A(B)*=C high-potential systems, at the reduced state, ($Q^{\bullet-}$) (an isocontour value of 0.0075 a.u. was used).

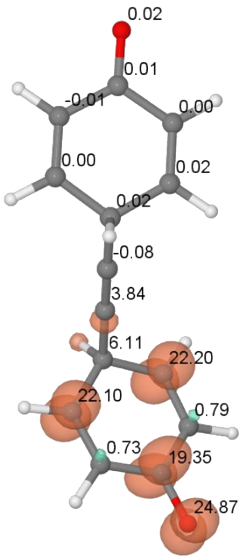

(a) CH−C≡C−CH

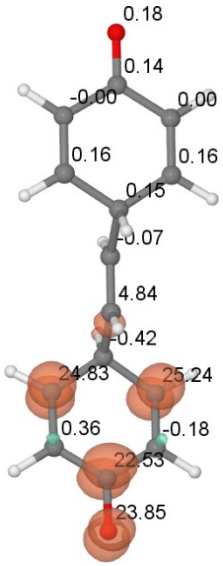

(b) CH−CH=CH−CH

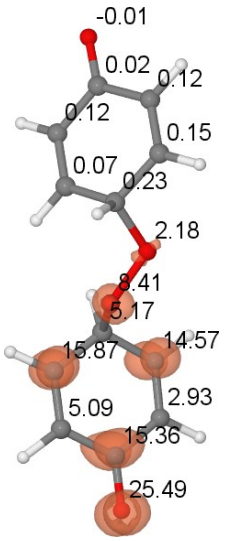

(c) CH−O-O−CH

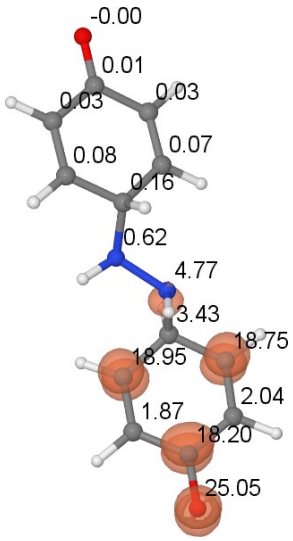

(d) CH−NH−NH−CH

Figure S9. Distribution of atomic spin density population in hundredths of electron for the C−*X*~*X*−C low-potential systems, at the reduced state, ($Q^{\bullet-}$) (an isocontour value of 0.0075 a.u. was used). In these molecules, the moiety below corresponds to the right moiety in Figure S10.

S7. Atomic charges according to the Bader's QTAIM framework

Tables S3 and S4 gather the whole set of atomic charges issued from QTAIM basins for both initial and reduced states. Additionally, Table S5 presents the sum of charge values associated with the bridges for the considered systems. Atom labelling for each system is mentioned in Figure S10:

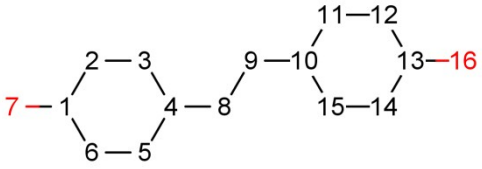

Figure S10. Atomic labelling used in Tables S3 and S4.

Atom	C=N−N=C		C=CH−CH=C		C=CH−N=C	
	Init.	Red.	Init.	Red.	Init.	Red.
C1	0.969	0.887	0.942	0.863	0.946	0.881
C2	0.050	-0.008	0.026	-0.043	0.025	-0.044
C3	0.084	0.007	0.046	-0.019	0.069	0.008
C4	0.650	0.475	0.010	-0.013	0.018	0.011
C5	0.082	0.010	0.050	-0.012	0.065	-0.016
C6	0.060	-0.003	0.024	-0.048	0.024	-0.067
O7	-1.159	-1.198	-1.180	-1.227	-1.178	-1.229
A8	-0.737	-0.675	0.072	-0.007	0.592	0.640
A(B)9	-0.737	-0.675	0.073	-0.007	-1.254	-1.291
C10	0.650	0.475	0.011	-0.015	0.646	0.473
C11	0.082	0.018	0.046	-0.018	0.079	0.007
C12	0.060	-0.022	0.028	-0.042	0.085	-0.030
C13	0.969	0.887	0.942	0.863	0.966	0.871
C14	0.050	-0.015	0.026	-0.043	0.080	-0.021
C15	0.084	0.026	0.046	-0.019	0.067	0.000
O16	-1.159	-1.198	-1.180	-1.227	-1.153	-1.195

Table S3. Atomic charges for the high-potential systems.

Atom	CH=O−O=CH		CH−C≡C−CH		CH−CH=CH−CH		CH=NH−NH=CH	
	Init.	Red.	Init.	Red.	Init.	Red.	Init.	Red.
C1	0.976	0.970	0.971	0.966	0.962	0.957	0.966	0.963
C2	0.037	0.025	0.033	0.026	0.014	0.007	0.026	0.022
C3	0.059	0.047	0.054	0.022	0.033	0.029	0.022	0.015
C4	0.563	0.565	0.225	0.425	0.135	0.135	0.425	0.430
C5	0.066	0.054	0.054	0.046	0.033	0.029	0.046	0.043
C6	0.046	0.032	0.033	0.018	0.014	0.007	0.018	0.014
O7	-1.180	-1.186	-1.191	-1.192	-1.197	-1.200	-1.192	-1.194
X8	-0.563	-0.598	-0.175	-0.308	0.008	-0.040	-0.308	-0.337
X9	-0.563	-0.502	-0.175	-0.311	0.008	-0.031	-0.311	-0.343
C10	0.559	0.353	0.225	0.440	0.136	0.089	0.440	0.339
C11	0.066	-0.078	0.054	0.025	0.033	-0.127	0.025	-0.130
C12	0.047	-0.079	0.033	0.017	0.014	-0.100	0.017	-0.100
C13	0.976	0.785	0.970	0.964	0.963	0.748	0.964	0.756
C14	0.037	-0.079	0.033	0.020	0.013	-0.099	0.020	-0.097
C15	0.058	-0.070	0.054	0.041	0.033	-0.128	0.041	-0.118
O16	-1.180	-1.237	-1.191	-1.191	-1.197	-1.265	-1.191	-1.256

Table S4. Atomic charges for the low-potential systems.

Bridge type	Ring 1			Ring 2		
	Initial	Reduced	Δ	Initial	Reduced	Δ
N−N	1.894	1.369	-0.525			
CH−CH	1.098	0.727	-0.371			
CH−N	1.864	1.299	-0.565	1.129	0.773	-0.356
C≡C	1.369	0.539	-0.830	1.369	1.339	-0.030
CH=CH	1.192	0.383	-0.809	1.191	1.164	-0.027
NH−NH	1.506	0.650	-0.856	1.506	1.486	-0.020
O−O	1.744	0.832	-0.911	1.744	1.693	-0.051

Table S5. Ring net atomic charges; Ring 2 values are present for cases presenting a dissymmetry between the two rings of the system (Ring 2 is the ring closer to the N−bridge in the C=CH−N=C system, while it refers to the unreduced ring in the *X*~*X* molecules).

S8. Energy partitioning based on Bader's QTAIM framework

For each analysed molecular entity (at both reduced and initial state), the energy was partitioned into chemical building blocks contributions based on Bader's QTAIM approach. These results are gathered in Table S5. Labelling bridge(4) and bridge(2) is respectively used to design the sums of the atomic energies by including or excluding the terminal atoms shared with the rings.

Bridge type	Atomic unit	Init. E	Red. E	ΔE
N−N	6MR	-229.933	-230.157	-0.224
	C=O	-113.368	-113.373	-0.005
	Bridge(4)	-185.767	-185.780	-0.013
	Bridge (2)	-110.316	-110.124	0.192
CH−CH	6MR	-230.380	-230.489	-0.109
	C=O	-113.395	-113.395	0.001
	Bridge(4)	-153.546	-153.579	-0.033
	Bridge(2)	-77.373	-77.402	-0.029
CH−N	6MR, close to N=C part of the bridge	-229.949	-230.191	-0.242
	6MR close to C=C part of the bridge	-230.365	-230.466	-0.101
	C=O, close to N=C part of the bridge	-113.383	-113.383	0.000
	C=O, close to C=C part of the bridge	-113.381	-113.385	0.004
	Bridge(4)	-170.263	-170.299	-0.036
	Bridge(2)	-93.859	-93.768	0.091
C≡C	6MR, reduced	-230.840	-231.023	-0.182
	6MR, unreduced	-230.840	-230.853	-0.012
	C=O, reduced	-113.397	-113.398	-0.001
	C=O, unreduced	-113.397	-113.380	0.017
	Bridge(4)	-153.507	-153.530	-0.023
	Bridge(2)	-76.338	-76.374	-0.036
CH=CH	6MR, reduced	-230.950	-231.116	-0.166
	6MR, unreduced	-230.950	-230.966	-0.016
	C=O, reduced	-113.403	-113.405	-0.002
	C=O, unreduced	-113.403	-113.384	0.019
	Bridge(4)	-154.673	-154.704	-0.031
	Bridge(2)	-77.380	-77.425	-0.046
NH−NH	6MR, reduced	-230.788	-230.985	-0.198
	6MR, unreduced	-230.788	-230.795	-0.006
	C=O, reduced	-113.395	-113.397	-0.002
	C=O, unreduced	-113.395	-113.381	0.014
	Bridge(4)	-187.951	-187.981	-0.029
	Bridge(2)	-110.975	-110.997	-0.022
O−O	6MR reduced	-230.600	-230.892	-0.292
	6MR, unreduced	-230.600	-230.630	-0.029
	C=O, reduced	-113.365	-113.368	-0.004
	C=O, unreduced	-113.365	-113.359	0.006
	Bridge(4)	-227.833	-227.842	-0.009
	Bridge(2)	-151.048	-150.954	0.094
Shortened bridge	6MR	-230.361	-230.491	-0.130
	C=O	-113.393	-113.392	0.001
C=$(CN)_2$ redox center	6MR	-230.549	-230.701	-0.153
	C=$(CN)_2$ red. cent.	-261.959	-261.990	-0.031
	Bridge(4)	-185.796	-185.809	-0.013
	Bridge(2)	-110.271	110.087	0.185

Table S6. Energy partitioning issued from the application of Bader's QTAIM approach.

S9. Bridge bond lengths and delocalization indices, δ

Bridge type	Bond length average			δ average			Bond length RMSD			δ RMSD		
	Init.	Red.	Δ	Init.	Red.	Δ	Init.	Red.	Δ	Init.	Red.	Δ
N−N	1.334	1.346	0.012	1.346	1.330	-0.016	0.001	0.002	0.001	0.003	0.114	0.110
CH−CH	1.397	1.412	0.015	1.373	1.327	-0.046	0.001	0.001	0.000	0.025	0.023	-0.002
CH−N	1.355	1.371	0.015	1.287	1.226	-0.061	0.002	0.006	0.004	0.024	0.011	-0.014
C≡C	1.387	1.393	0.006	1.560	1.550	-0.010	0.046	0.048	0.002	1.753	1.756	0.003
CH=CH	1.461	1.465	0.004	1.234	1.228	-0.006	0.023	0.024	0.001	0.442	0.440	-0.002
NH−NH	1.465	1.477	0.013	1.011	0.994	-0.017	0.002	0.000	-0.002	0.038	0.044	0.007
O−O	1.452	1.490	0.037	0.946	0.927	-0.019	0.001	0.006	0.005	0.070	0.090	0.020

Table S7. Bridge bond lengths and delocalization indices, δ.

References

1. Gaussian 09, Revision D.01 M. J. Frisch, G. W. Trucks, H. B. Schlegel, G. E. Scuseria, M. A. Robb, J. R. Cheeseman, G. Scalmani, V. Barone, B. Mennucci, G. A. Petersson, H. Nakatsuji, M. Caricato, X. Li, H. P. Hratchian, A. F. Izmaylov, J. Bloino, G. Zheng, J. L. Sonnenberg, M. Hada, M. Ehara, K. Toyota, R. Fukuda, J. Hasegawa, M. Ishida, T. Nakajima, Y. Honda, O. Kitao, H. Nakai, T. Vreven, J. A. Montgomery, Jr., J. E. Peralta, F. Ogliaro, M. Bearpark, J. J. Heyd, E. Brothers, K. N. Kudin, V. N. Staroverov, R. Kobayashi, J. Normand, K. Raghavachari, A. Rendell, J. C. Burant, S. S. Iyengar, J. Tomasi, M. Cossi, N. Rega, J. M. Millam, M. Klene, J. E. Knox, J. B. Cross, V. Bakken, C. Adamo, J. Jaramillo, R. Gomperts, R. E. Stratmann, O. Yazyev, A. J. Austin, R. Cammi, C. Pomelli, J. W. Ochterski, R. L. Martin, K. Morokuma, V. G. Zakrzewski, G. A. Voth, P. Salvador, J. J. Dannenberg, S. Dapprich, A. D. Daniels, O. Farkas, J. B. Foresman, J. V. Ortiz, J. Cioslowski and D. J. Fox, Gaussian, Inc., Wallingford CT, 2009.
2. A. V. Marenich, C. J. Cramer and D. G. Truhlar, *J. Phys. Chem. B*, 2009, **113**, 6378.
3. J. M. Vollmer, L. A. Curtiss, D. R. Vissers and K. Amine, *J. Electrochem. Soc*., 2004, **151**, A178.
4. A. D. Becke, *J. Chem. Phys.*, 1993, **98**, 5648.
5. C. Lee, W. Yang, and R. G. Parr, *Phys. Rev. B*, **37** (1988) 785.
6. J. Kruszewski and T. Krygowski, *Tetrahedron Lett.*, 1972, **13**, 3839.
7. X. Fradera, M. A. Austen and R. F. W. Bader, *J. Phys. Chem. A*, 1999, **103**, 304.
8. E. Matito, M. Duran and M. Solà, *J. Chem. Phys.*, 2005, **122**, 014109.
9. F. Feixas, E. Matito, J. Poorter and M. Solà, *J. Comput. Chem.*, 2008, **29**, 1543.
10. R. F. W. Bader, *Atoms in Molecules: A Quantum Theory*, Clarendon Press, Oxford, 1994
11. C. Gatti, SF-ESI codes, private communication.